

Slab-fluids contain chlorine

KAWAMOTO, Tatsuhiko^{1*}

¹Institute for Geothermal Sciences, Kyoto University

We found that the fluid inclusions of sub-arc mantle peridotites have 5.1 wt. % NaCl beneath the Pinatubo, a frontal volcano (Kawamoto et al., 2013 PNAS) and 3.7 wt. % NaCl beneath the Ichino-megata, a rear-arc volcano (Kumagai et al., under review). Based on these observations, we suggest that the slab-derived fluids are saline fluids.

In order to understand the effects of salinity on the arc-magma chemistry, two series of elemental partitioning experiments between silicate melts and aqueous fluids have been carried out with and without Cl in synchrotron facilities. The experiments show that highly saline fluids can transfer Pb, Rb, and Cs more effectively than Sr and Ba from subducting oceanic lithosphere to the mantle wedge. As suggested by Keppler (1996, *Nature*), saline fluids can be an important agent to transfer large ion lithophile elements. Geochemical studies have suggested that three chemical components are involved in the formation of arc-basalts: the depleted mantle, aqueous fluid, and melt components (Pearce et al., 2005 *G-cube*). If supercritical fluids contain Cl and then subsequently separate into aqueous fluids and melts (Kawamoto et al., 2012, PNAS), then it follows that such aqueous fluids will inherit much of the Cl and also some of the large ion lithophile elements to explain qualitatively the geochemical features of Mariana arc basalts. In contrast, Cl-free aqueous fluids may not be able to transfer Pb to the magma source. Our partitioning experiments were conducted using highly saline fluids (12-25 wt % (Na, K)Cl). Based on the geochemical features, slab-fluids are likely to contain Cl, although their amount remains to be quantified.

References

Kawamoto T., Kanzaki M., Mibe K., Matsukage K.N., Ono S. (2012) Separation of supercritical slab-fluids to form aqueous fluid and melt components in subduction zone magmatism. *Proc. Nat. Acad. Sci. USA* 109, 18695-18700.

Kawamoto T., Yoshikawa M., Kumagai Y., Mirabueno M.H.T., Okuno M., Kobayashi T. (2013) Mantle wedge infiltrated with saline fluids from dehydration and decarbonation of subducting slab. *Proc. Nat. Acad. Sci. USA* 110, 9663-9668.

Keppler H. (1996) Constraints from partitioning experiments on the composition of subduction-zone fluids. *Nature* 380, 237 - 240.

Pearce J.A., Stern R.J., Bloomer S.H., Fryer P. (2005) Geochemical mapping of the Mariana arc-basin system: Implications for the nature and distribution of subduction components. *Geochem. Geophys. Geosys.* 6, Q07006.

Keywords: subduction zone, H₂O, fluid inclusion, mantle wedge, synchrotron X-ray, magma

Numerical modeling of water-rock reaction with a focus on the earth's surface environment

YOKOYAMA, Tadashi^{1*}

¹Osaka University, Graduate School of Science, Department of Earth and Space Science

Water-rock interaction proceeds by the interplay between dissolution/precipitation, diffusion of ions, and water flow in rock pores. The reaction-transport process in rock is quantitatively described by:

$$\phi(\partial c/\partial t) = D_e(\partial^2 c/\partial x^2) - v\phi(\partial c/\partial x) + Ar_0f(c)$$

This equation is an example of the one-dimensional reaction-transport equation, and c is the solute concentration (mol/cm³), t is the time (s), x is the distance (cm), ϕ is the porosity (dimensionless), D_e is the effective diffusion coefficient (cm²/s), v is the flow rate in pores (cm/s), A is the surface area per unit volume of rock (cm²/cm³), r_0 is the rate constant (mol/cm²/s). $f(c)$ is the function that expresses the concentration dependence of the dissolution rate (mol/cm²/s), and for quartz, $f(c) = (1 - c/c_{eq})$ (c/c_{eq} is the equilibrium Si concentration) (Scott et al., 2009). By solving the reaction-transport equation, we can know how the distributions of the solute concentration and dissolution rate and the amounts of primary and secondary minerals change with time. Such analysis is called the reactive transport modeling and has been applied to the studies of various processes including soil formation (Maher et al., 2009) and the reactions associated with geologic storage of CO₂ (Xu et al., 2010).

The parameters used in the reaction-transport equation can be estimated by direct measurement in the field, laboratory experiment, and fitting in the modeling. To reproduce natural process accurately, we need to estimate each parameter as precisely as possible. However, it is difficult to evaluate what value is most proper. For example, the reactive surface area A is often determined by measuring the volume of gas adsorbed on the mineral or by approximating the geometry of the mineral. However, the proportion at which the reactive surface area determined by these processes contributes to actual reaction is often unclear. In addition, there are cases where various $f(c)$ have been proposed for a specific mineral and the dissolution rate varies with time (White and Brantely, 2003). In such case it is unclear what equation should be used. Therefore, the way of setting appropriate parameter is one of the main subjects of research.

In water-rock reaction on the earth's surface environment, evaluation of the effect of water saturation is important because water saturation changes dynamically as a result of the occurrence of intermittent drying and infiltration. It has been reported that both the hydraulic conductivity and effective diffusion coefficient in rock decrease with decreasing water saturation and this significantly affects the result of the reactive transport modeling (Yokoyama, 2013). In addition, how water saturation affects the reactive surface area has been revealed recently (Nishiyama and Yokoyama, 2013).

Keywords: Reactive transport modeling, Water-rock reaction

Kinetics of overall silica precipitation within the Earth's crust

SAISHU, Hanae^{1*}; OKAMOTO, Atsushi²; TSUCHIYA, Noriyoshi²

¹AIST, ²Tohoku University

The kinetics of dissolution and precipitation of silica minerals is important to reveal the geochemical reaction and to estimate how long silica deposits forms in the Earth's crust. The present kinetic equation for silica-water reactions was determined at 0-300 C and in the low Si saturated solution, where quartz growth on quartz surfaces occurs than that of nucleation of silica polymorphs [1]. However, the precipitation experiments of the high Si supersaturated solution showed that the co-precipitation of silica polymorphs via nucleation could occur [2], and the euhedral quartz crystals precipitates without precursor of silica polymorphs from the solution with minor components (Al and Na) [3].

In this study, the overall precipitation rate of silica minerals, which includes surface reaction of quartz (first term) and nucleation of silica polymorphs (second term), is derived empirically to estimate the total amount of silica precipitation within the Earth's crust. The previous kinetic equation of surface reaction [1] is applied as the first term. Based on the precipitation experiments of flow rate, the nucleation-controlled precipitation of silica minerals is expressed in a first order rate equation in the second term. The applicability of the nucleation term determined as the nucleation parameter is only in the conditions that precipitation occurs: in the solution supersaturated with respect to quartz, and in the supercritical conditions of water. The rate constant of nucleation is derived as a function of Al concentration in the solution based on the experiments of silica precipitation [3].

By using the new kinetic equation, silica-water interaction was simulated at the well WD-1a of the Kakkonda geothermal field, Japan, which penetrated the boundary of the hydrothermal convection and heat conduction zones [4]. Amount of dissolution and precipitation of silica minerals increases with decreasing of the fracture permeability. The largest amount of silica precipitation occurs in the downflow fluid at the permeable-impermeable boundary regardless of the fracture permeability.

The equilibrium consideration [5] and the kinetic results indicate that, if open fractures forms at the depth of the permeable-impermeable boundary, the impermeable zone could be reproduced by precipitation of silica minerals, which cause the sustainable division between the permeable zone and the impermeable zone in the Earth's crust.

References

- [1] Rimstidt and Barnes (1980) *Geochim. Cosmochim. Acta*, **44**, 1683-1699.
- [2] Okamoto et al. (2010) *Geochim. Cosmochim. Acta*, **74**, 3692-3706.
- [3] Saishu et al. (2012) *Am. Min.*, **97**, 2060-2063.
- [4] Doi et al. (1998) *Geothermics*, **27**, 663-690.
- [5] Saishu et al. (in press) *Terra Nova*.

Keywords: Silica precipitation, Hydrothermal experiment, Kinetic equation, Nucleation, Permeable-impermeable boundary

Sedimentary pore-fluid origin of H₂O-rich fluid in mantle wedge revealed by halogens and noble gases

KOBAYASHI, Masahiro^{1*}; SUMINO, Hirochika¹; NAGAO, Keisuke¹; ISHIMARU, Satoko²; ARAI, Shoji³; YOSHIKAWA, Masako⁴; KAWAMOTO, Tatsuhiko⁴; KUMAGAI, Yoshitaka⁴; KOBAYASHI, Tetsuo⁵

¹GCRC, Univ. Tokyo, ²Dept. Earth Environ. Sci., Kumamoto Univ., ³Dept. Earth Sci., Kanazawa Univ., ⁴Inst. Geothermal Sci., Kyoto Univ., ⁵Dept. Earth Environ. Sci., Kagoshima Univ.

H₂O plays an important role in mantle processes in subduction zones. Yet its subducting processes to the mantle remain unknown because of scarcity of direct observations of H₂O in mantle-derived materials. Since halogen and noble gas are strongly partitioned into fluids and they show distinct elemental and/or isotopic ratios depending on their origins, their compositions in mantle rocks can provide complementary constraints on the behavior and origin of H₂O in the mantle. Although only few researches have been conducted, the subduction of halogens and noble gases derived from sedimentary pore fluids (seawater trapped in pores of deep-sea sediments) has been suggested. Pore fluid-like halogens and noble gases were found in mantle wedge peridotites which captured H₂O-rich fluids just above a subducting slab [1]. H₂O-rich fluid inclusions whose salinity is similar to that of pore fluids (salinity of pore fluids is the same level as that of seawater [2]) are found in a mantle xenolith from a subduction zone [3]. We investigated halogen and noble gas compositions of mantle wedge peridotites from subduction zones to better constrain how far the influence of subducted sedimentary pore fluids extends into the mantle.

The samples studied are harzburgitic xenoliths from the Avacha volcano in Kamchatka and the Pinatubo volcano in the Philippines, and alpine-type peridotite from the Horoman massif in Japan. H₂O-rich fluid inclusions have been found in olivine of those mantle peridotites [3,4,5].

We applied the noble gas method, in which halogens (Cl, Br, and I) are converted to corresponding isotopes of Ar, Kr, and Xe by neutron irradiation in a nuclear reactor and then the concentrations of noble gas isotopes are determined by noble gas mass spectrometry. Halogen detection limits of this method are from two to five orders of magnitude lower than conventional method, which enable to determine the low halogen abundances in mantle-derived materials. By crushing samples under ultra-high vacuum, noble gases are selectively extracted from H₂O-rich fluid inclusions. Unirradiated peridotites were also analyzed to obtain precise noble gas isotope compositions.

The halogens of all peridotites are heavily enriched in I, although the halogen ratios are distinctive in each locality. These high I/Cl ratios show a strong contribution of sedimentary pore fluids [2]. The noble gases except for He have the elemental and isotopic ratios similar to elementally fractionated atmospheric noble gases dissolved in seawater, which is probably equivalent to those dissolved in sedimentary pore fluids. The ³He/⁴He ratios are similar to that of the mantle and distinctly higher than the atmospheric ratio. This indicates that the fluids derived from subducting slabs acquired He from the ambient mantle, where He is much more enriched than in seawater.

These pore fluid-like halogen and noble gas signatures are strong evidence that the H₂O-rich fluids in the studied peridotites are derived from sedimentary pore fluids and transported to the mantle.

References: [1] Sumino *et al.* (2010) *EPSL* **294**, 163. [2] e.g. Muramatsu *et al.* (2007) *Appl. Geochem.* **22**, 534. [3] Kawamoto *et al.* (2013) *PNAS* **110**, 9663. [4] Ishimaru *et al.* (2007) *J. Petrol.* **48**, 395. [5] Arai & Hirai (1985) *Nature* **318**, 276.

Keywords: water, halogen, noble gas, subduction zone, mantle, peridotite

Relations among temperature, dehydration of the PHS plate, and a large earthquake, a SSE, and LFEs in the Tokai district

SUENAGA, Nobuaki^{1*} ; YOSHIOKA, Shoichi² ; MATSUMOTO, Takumi³

¹Graduate School of Science, Kobe Univ., ²RCUSS, Graduate School of Science, Kobe Univ., ³NIED

In this study, we performed numerical simulations of temperature distribution at the plate boundary and estimated the dehydration process of hydrous mid ocean ridge basalt (MORB) in the oceanic crust in the Tokai district, central Japan. We discuss the relationships among temperature, dehydration, and a future megathrust earthquake, deep low-frequency earthquakes (LFEs), and a slow slip event (SSE). Our results identified a strongly coupled region for an expected megathrust Tokai earthquake based on temperature conditions at the plate boundary. The depth range of the plate boundary where the megathrust earthquake may occur is 9~21 km, narrowing toward the east. An SSE is estimated to have occurred in the transition zone between unstable and stable sliding. Hypocentral depths of LFEs deviating from the isodepth contours of the Philippine Sea plate toward the east may be explained by differences in the dehydration process associated with phase transformations in hydrous MORB.

Keywords: 2-D thermal modeling, megathrust earthquake, low-frequency earthquake (LFE), slow slip event (SSE), temperature, dehydration from hydrous MORB

The regional and single-vein scale distribution of the CO₂ fluids in the Shimanto accretionary complex, Muroto area, SW

MUSHA, Michimasa^{1*}; TSUCHIYA, Noriyoshi¹; OKAMOTO, Atsushi¹

¹Environmental Studies of Tohoku University

Carbon dioxide and methane are major carbonic components of the fluids in the crust. The crustal fluids generally have composition of C-H-O system, mainly composed of H₂O, CO₂, and CH₄, and they may be carried down into Earth's interior at subduction zones. Many studies have examined fluid components in various accretionary prisms under low-grade metamorphic conditions, and CH₄ is showed as the only carbonic species. Therefore, there is little information on the variation of the components of C-H-O fluids in subduction zones.

The Tertiary (Paleogene and Neogene system) Shimanto belt, southwest in Japan, is one of the best-studied ancient accretionary complexes. The Muroto Peninsula belongs to the Tertiary Shimanto belt, and it is mainly composed of sandstones, mudstones and conglomerates with small amount of basalt. Mineral veins were mainly composed of quartz, with small amount of calcite near the vein walls, while many studies have showed CH₄ is the only carbonic component in the Shimanto belt, therefore it is unclear why calcite precipitated in the veins in absence of CO₂. Lewis (2000) reported the fluid inclusions of CH₄ and CO₂ mixture at one area in the Muroto Peninsula, but the extensive distribution of CO₂ fluids in the whole peninsula is not clear. In this study, we examined the distribution of C-H-O fluids from the Muroto Peninsula, as fluid inclusions in the mineral veins, using microthermometry and Laser Raman spectroscopy, in regional scale and single vein scale.

Fluid inclusions from quartz in the veins are composed of one-phase carbonic inclusions (only CH₄) and two-phase aqueous inclusions (carbonic vapor and H₂O liquid). Carbonic components of the vapor phase in the two-phase inclusions are gradually transitioned from CH₄-dominant in the north area of the belt to a CO₂?CH₄ mixture in the south; the CO₂/(CO₂ + CH₄) ratio in mole fraction (X_{CO_2}) vary from 0 ~0.3 in the north area to 0 ~0.9 in the south.

In single vein scale, we examined single CO₂-bearing vein from the south area of the Peninsula, where X_{CO_2} is 0 ~0.8. The CO₂ ratio in the carbonic species is decreased from the vein wall ($X_{CO_2} = 0.5$?0.8) to the vein center, in which carbonic species in the fluids is only CH₄ ($X_{CO_2} = 0$). The existence of CO₂ only near the vein walls is in good agreement of the precipitation of calcite near the vein walls. The homogenization temperature increases from ~180 °C to 240?250 °C, indicating the transition of the carbonic species from CO₂?CH₄ to CH₄ during vein formation.

The dominant species of carbonic species in most accretionary prisms is CH₄ under low-grade metamorphic conditions, and thermodynamic calculation about equilibrium in the C-H-O fluids also shows that CH₄ is dominant carbonic species in the equilibrium with graphite under the P?T conditions of formation of the CO₂-bearing veins (235?245 °C, 165?200 MPa). The CO₂-fluids are preferentially distributed close to an out-of-sequence thrust that brings the Muroto sub-belt into contact with the late Oligocene?early Miocene Nabae sub-belt with its many volcanic lavas and intrusive rocks. Therefore, the CO₂-fluids were considered to be magmatic-origin, and that the fluids were injected and mixed with the CH₄-pore-fluids of the sediments in the accretionary prism in the timing of formation of CO₂-bearing veins.

Keywords: fluid inclusions, accretionary complexes, calcite, mineral veins, C-H-O fluid, Shimanto belt

Visualization of deep-seated fluid flow in Tokusa Basin, Yamaguchi Prefecture

NISHIYAMA, Nariaki^{1*}; TANAKA, Kazuhiro²; SUZUKI, Koichi³

¹Yamaguchi University, ²Yamaguchi University, ³Central Research Institute of Electric Power Industry

It is known that highly saline fluids spout out in spite of inland area in Japan (Sakai et al. 1978). These fluids spout out not only at the surface of the ground surface but also at the flowing borehole. However, the erupted region of ascending fluid from flowing borehole and its relationship to the geological structure is not identified. Electromagnetic surveys applying Controlled Source Audio-frequency Magneto-Telluric Method was carried out in the Tokusa basin, Yamaguchi Prefecture to obtain the two dimensional distribution of resistivity to clarify the geological structure and the distribution of deep-seated fluid.

The study area is consisted of the Late Cretaceous welded tuff, rhyolitic lava, and the Holocene sediments. Low resistivity zone continuously is distributed along the Tokusa-Jifuku fault (Sagawa et al, 2008) in bedrock more than 2.5km long and is distributed in north side of the fault in sediments like a tongue shape. Resistivity of erupted highly saline water corresponds to that obtained by CSAMT. Groundwater of the shallow wells drilled in the sediments shows the NaCl type. Therefore, low resistivity zone in the sediments corresponds to the highly saline water diluted by surface groundwater. As a result, deep-seated fluid in the Tokusa basin rises along the Tokusa-Jifuku fault in the basement rock and then flows to river subjected to the dilution by surface groundwater.

Keywords: Deep-seated fluid, CSAMT method, Tokusa-Jifuku fault, Groundwater flow

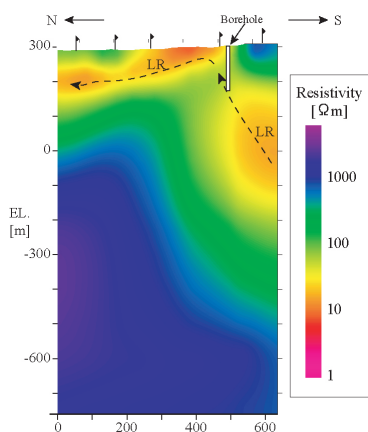


Fig.1 The resistivity profile by the CSAMT survey.

Can clay minerals account for the non-asperity on the subducting plate interface?

KATAYAMA, Ikuo^{1*}; KUBO, Tatsuro¹; SAKUMA, Hiroshi²; KAWAI, Kenji³

¹Department of Earth and Planetary Systems Science, Hiroshima University, ²National Institute for Materials Science, ³Department of Earth and Planetary Sciences, Tokyo Institute of Technology

Seismicity along the subducting plate interface shows a regional variation, in which large earthquakes occur repeatedly at the strongly coupled patches that are surrounded by weakly coupled regions. This model suggests that the subduction plate interface is heterogeneous in terms of frictional properties; however, mechanism making the difference in strong and weak coupling is still not well understood. We consider this difference to relate to the alternation of plate interface due to aqueous fluids that result in the spatial distribution of clay minerals. In this study, we measured the frictional healing of clay minerals and discuss whether the frictional properties of clays can account for the weakly coupled non-asperity regions in the subducting plate interface.

We carried out a series of slide-hold-slide frictional experiments to examine the time-dependent frictional restrengthening of the simulated fault gouge. In the experiments, the axial loading was interrupted for periods ranging 10 to 3000 s after steady-state friction, and we measured the difference between the steady-state friction and the peak friction after each holding period. Mechanical data were recorded continuously with a sampling rate of 10 Hz and the frictional coefficient was calculated from the shear force divided by the normal force assuming zero cohesion.

The preliminary results show that the frictional strength of clay minerals (smectite and chlorite) slightly increases with holding time; however, the healing rate is significantly smaller than that of dry silicates such as quartz. Similar weak healing rate has been reported in the serpentized simulated faults (Katayama et al., 2013). These experimental results suggest that the recovery of fault strength is different in materials, in which clay minerals show weak and slow recovery whereas dry materials show relatively quick and thereby strong coupling on the fault surface. Aqueous fluids that are released from the descending plate may change the mineralogy on the plate interface where clay minerals become dominant at the channel of fluid flow surrounding the unaltered dry patches that potentially act as a seismic asperity. Thus, the heterogeneous fluid pathway and spatial distribution of clay minerals may play a key role for the formation of asperity and non-asperity on the subducting plate interface.

Keywords: Interplate earthquake, Asperity, Clay minerals, Frictional experiment, Frictional healing

Oxidation state of arc primary magma-inferred from sulfur speciation of melt inclusions

SHIMIZU, Kenji^{1*}; KASHIWABARA, Teruhiko¹; TAMENORI, Yusuke²

¹JAMSTEC, ²JASRI, SPring-8

Oxidation state of arc magmas highly influences the chemical behaviors of redox sensitive elements such as chalcophile and some siderophile elements in subduction zone. Therefore, Oxidation state of arc magmas is essential to understand arc magma geneses and evolutions of ore deposits. It has been suggested that sub-arc mantle is oxidized by subducted materials such as fluid, sediments and oceanic crust. However, recent studies contradicted that the oxidation state of primary arc magma (sub-arc mantle) is similar to the average upper mantle and oxidation is caused by differentiation associated with crystallization and interaction within preexisting crust (e.g. Lee et al., 2012, Science, v336, p64).

In order to constrain oxidation state of primary arc magmas at an immature subduction zone, we have analyzed $S_{6+}/\Sigma S$ of boninitic and tholeiitic melt inclusions within Cr-spinel from Bonin Islands and Guam by soft X-ray microbeam at SPring-8/BL27SU. Boninite in Bonin Islands uniquely formed at the early stage of subduction formation (~50 Ma) by melting of highly depleted hydrous mantle and 0-7 myrs later, related arc tholeiites erupted in southern Bonin Islands and Guam by melting of depleted mantle (Ishizuka et al., 2011, EPSL, v306, p229). Compositions of melt inclusions fully cover compositional ranges of whole-rocks and some boninitic melt inclusions have MgO higher than 20 wt%, showing that they are very primitive magmas. $S_{6+}/\Sigma S$ of boninitic and tholeiitic melt inclusions are 0.57 to 0.78 and 0.47 to 1, respectively; $S_{6+}/\Sigma S$ of all high-MgO (7 to 12 wt%) tholeiitic melt inclusions are >0.9. Oxygen fugacities of primary boninite and tholeiite are estimated to be $\Delta FMQ >+1$ and $>+1.5$, respectively by experimental results of Jugo et al. (2010, GCA, v74 p5926), indicating that sub-arc mantle is oxidized even at an early stage of subduction zone. Between the period of eruption of boninite and tholeiite, not only mantle sources but also the subducting component in term of oxidation state of sub-arc mantle may have changed.

Keywords: melt inclusion, boninite, arc, sulfur

Evaluating slab-fluid contribution into inhomogeneous mantle source: geochemical variation of Central and East Java arc

HANDINI, Esti^{1*} ; HASENAKA, Toshiaki¹ ; WIBOWO, Haryo edi² ; SHIBATA, Tomoyuki³ ; MORI, Yasushi⁴ ; HARIJOKO, Agung²

¹Graduate School of Science and Technology, Kumamoto University, ²Geological Engineering, Gadjah Mada University, ³Institute for Geothermal Sciences, Kyoto University, ⁴Kitakyushu Museum of Natural History and Human History

The spatial distribution of the volcanoes in Central and East sections of Java arc denotes the widest and the narrowest of Java Island. Central Java section corresponds to the largest range and depth of Wadati-Benioff Zone along the island (180-360 km), whereas East Java section shows the narrowest range (190-220 km). However, both sections equally show wide geochemical variation with the function of slab-depth. Both also mark the appearance of the rear-arc alkaline suites in a different slab depth (360 km for Central Java, and 220 km for East Java). Geochemical datasets of basalt to basaltic andesite (further screened on Zr/Nb basis) from these sections were compiled to evaluate the contributions of slab-derived fluid to the mantle sources, and to assess the possible mantle sources of these magmas.

We group the lavas of the Central and East Java into two series: (1) the volcanic front series (VF), calc-alkaline suites of frontal- and middle-arc region volcanoes of Central and East Java, and (2) the rear-arc series (RA) consists of alkaline suites from Central and East Java (Muria, and Ringgit-Beser and Lurus, respectively). The VF series consistently shows typical island arc geochemistry, with strong LILE enrichment (Sr, Ba, Pb, and Rb) relative to HFSE. The RA series, mainly Muria, indicate stronger enrichment of LILE than other volcanoes closer to the trench. Ringgit-Beser and Lurus, the rear-arc lavas of East Java, behave differently in LILE enrichment. Ringgit-Beser lavas shows stronger LILE enrichment than that of lavas from Lurus, within the same enrichment range of Muria lavas. In the other hand, Lurus lavas are showing obvious HFSE depletion compared to OIB. The decreasing trend of LILE/HFSE and LILE/LREE (e.g. Ba/Nb, Ba/La, Pb/Ce, Pb/Nb) is observed across both Central and East Java sections. These ratios become lower toward the rear-arc of both sections, and the lowest in the rear-arc of Central Java. In various normalized plots (such as Nb vs. Ba/Nb), the VF series are plotted within the range of typical island arc basalts (IAB). Muria lavas, the rear-arc alkaline suite of the Central Java, resemble OIB and other non-arc type alkaline rock characteristics, but with positive indications of being island arc, such as negative Nb and Ti anomalies. Ringgit-Beser and Lurus alkaline lavas of East Java, however, are associated with other arc-type alkaline rock characteristics, with stronger signature of island arc than Muria.

Our analyzed samples show that lavas from East Java are closer in compositions to primitive magmas compared to Central Java's. The thicker overriding crust beneath Central Java than East Java possibly acts as the magma retainer that allows extensive fractionation. Across-arc variation of slab-derived fluid in both sections are observed as shown by decreasing LILE/HFSE and LILE/LREE toward rear-arc, suggesting the decreasing amount of slab-fluid added to the great slab-depth. The slab-fluid added to the volcanic front of East Java is slightly higher than that of Central Java, which may be controlled by the narrow range of slab dehydration area in the former that allows more fluid to concentrate. The low ratio of these trace elements in the rear-arc of both sections suggests that these parts have also been affected by dehydration of subducted slab. The stronger slab-fluid contributions in the rear-arc alkaline lavas of East Java than that of Central Java may reflect the role of shallower slab depth. Different mantle characteristics between the rear-arc of Central and East Java may reflect several possibilities: (1) the inhomogeneous mantle plume (E-type/EMI) beneath both sections, or (2) stronger EMI-type mantle contribution to Central Java than to East Java, or (3) the combination of both.

Keywords: Sunda arc, slab-derived fluid, across- and along-arc variations, trace elements

Reaction progress and porosity change in hydrothermal alternation at Olivine/Quartz boundary

OYANAGI, Ryosuke^{1*}; OKAMOTO, Atsushi¹; TSUCHIYA, Noriyoshi¹

¹Graduate School of Environmental Studies, Tohoku University

Serpentinization in oceanic lithosphere is a fundamental process to bring water into deep earth's interior. It is known that silica activity controls the reaction paths during the hydrothermal alternation of peridotites [e.g. 1,2], however the detailed reaction mechanism induced by silica transport is poorly understood. In this study, we conducted hydrothermal experiments in olivine (Ol)-quartz (Qtz)-H₂O system for investigating the mechanism of silica metasomatism at crust/mantle boundary.

Composite powders, which was composed of Qtz zone and Ol zone was set in inner tubes, with diameters of 1.7 mm and heights of 50 mm, and then loaded into autoclave with alkaline solution (NaOH, aq, pH = 13.8 at 25 °C). Temperature and pressure are 250 °C and vapor-saturated pressure (= 3.98 MPa), respectively. After the experiments, the inner tube was cut into ten segments to evaluate the reaction progress as a function of the distance from Ol/Qtz boundary (hereafter denoted X), by Thermogravimetry and XRD. In order to evaluate the spatial variation of the reactions, the area of each minerals (olivine and reaction products) and pore was measured from the back-scattered electron (BSE) images of the thin section.

After 46 days, the H₂O content near the Ol/Qtz boundary is lower (3.9 wt.% H₂O) than that in (12 wt.%) at the margin of the reaction tube. The reaction products after olivine changed systematically as away from Ol/Qtz boundary from smectite+serpentine zone to the serpentine+brucite zones. In the smectite+ serpentine zone, the (Mg+Fe)/Si ratio of the products increases from 0.5 to 1.5, indicating that proportion of serpentine with respect to smectite increased away from the boundary. With increasing time, the smectite+ serpentine zone was enlarged, where as the serpentine+brucite zones was retreated.

Based on the combined analyzes of BSE images, TG and SEM-EDS, we obtained the reaction progresses of individual elementary reactions between 25 and 46 days as follows:

(1) In the smectite+ serpentine zone, smectite was formed via hydration of olivine and dehydration of serpentine by supply of silica. As the result, overall reaction has a variation in the smectite+ serpentine zone; ΔmH_2O is negative (hydration) at X=0-4 mm, it is positive (dehydration) at X=4-10 mm. Volume expansion factor (V/V₀) is much higher (=1.4) at Ol/Qtz boundary than other zones (=1.1), mainly due to Si-metasomatic reaction.

(2) Far from the Ol/Qtz boundary (X = 20-40 mm), there is no influence of silica supply, indicating that silica was completely consumed in the smectite+ serpentine zone. In these area, serpentinization proceeds as the typical olivine hydration reaction to produce brucite and serpentine with constant Srp/Brc ratio.

(3) In the transient zone, serpentine was formed by two ways: hydration of olivine and dehydration of brucite by supply of silica. These two serpentine forming reaction resulted in a large amount of serpentine in this area, and high volume expansion factor (=1.4).

Due to these two volume expansion reactions, low porosity (~5%) area developed locally, never-theless porosity of other area is 30%. The amount of silica ($\Delta mSiO_2$, aq), which consumed from 25 to 46days, is largest at Ol/Qtz boundary, and monotonically decreases with increasing distance. If excess silica are available, the zones affected by silica will increase gradually with increasing time during hydrothermal alteration around mantle/crust boundary. In contrast, the porosity has a minimum around X = 15 mm in the transition zone, because Ol-hydration and Brc-dehydration reaction proceed with large volume expansion. Such volume expansion reaction and mineral changes causes the mechanical strength of boundary.

References:

- [1] Frost, B. R., & Beard, J. S. (2007). *Journal of Petrology*, 48(7), 1351-1368.
- [2] Ogasawara, Y., Okamoto, A., Hirano, N., & Tsuchiya, N. (2013). *Geochimica et Cosmochimica Acta*, 119, 212-230.

Keywords: serpentinization, ultramafic rock, Si-metasomatism, Hydrothermal alternation

Distribution and transportation of melt in subduction zones

ISHII, Kazuhiko^{1*}

¹Graduate School of Sciences, Osaka Prefecture University

Volcanic and seismic activities in subduction zones are the result of complex interaction of geophysical and geochemical processes. I have investigated the hydration and dehydration and the generation and transportation of melt in subducting slab and adjacent mantle wedge using a numerical model. The model includes hydration and dehydration of the slab and mantle wedge, melting and solidification of mantle peridotites, permeable flow of melt and aqueous fluids, and solid flow of mantle peridotites with water- and melt-induced weakening. The model shows the melt distribution in the mantle wedge beneath the volcanic front and extending sub-parallel with the subducting slab. The detailed geometry of the melt distribution is strongly dependent on the parameters including water solubility of peridotites and permeable flow velocities of melt and aqueous fluids. I will discuss the effect of these parameters on the melt distribution and the interdependence among the geodynamic processes in the subduction system.

Keywords: subduction zones, melt, distribution and transportation

Effects of mineral grain size variation on fluid migration in the mantle wedge

WADA, Ikuko^{1*} ; BEHN, Mark D.²

¹IRIDeS, Tohoku University, ²Woods Hole Oceanographic Institution, USA

In this study, we investigate the effect of mineral grain size on the migration paths of aqueous fluids in the mantle wedge. Grain size is an important parameter that controls the grain-scale permeability of the mantle; in general, the smaller the grain size, the less permeable the mantle is, provided that the pores between grains are connected. The migration paths of aqueous fluids are therefore dependent on the grain size distribution, influencing the location and the degree of hydrous melting in the mantle wedge and the location of arc volcanism. We develop a 2-D fluid migration model with generic subduction zone geometry. In the model, we adopt grain size distributions calculated by coupling a subduction zone thermal model with a laboratory-derived grain size evolution model for a range of subduction parameters (Wada et al., 2011). The fluid migration model also includes the effects of mantle flow velocities and mantle-flow-induced pressure gradients, both of which are also calculated from the thermal model. The calculated grain size immediately above the slab is on the order of 10²-100 micrometers beneath the forearc region, depending on the slab thermal structure, and it increases down-dip to a few cm beneath the arc region. Our preliminary modeling results with a simplified fluid influx pattern indicate that the aqueous fluids tend to become trapped in the down-going mantle due to low permeability and dragged down-dip until permeability becomes high enough for the fluids to migrate upward. Grain size above a colder slab tends to be smaller than that above a warmer slab, and therefore fluids become dragged down-dip further in a cold-slab subduction zone than in a warm slab subduction zone. A colder slab also tends to release fluids at deeper depths than a warmer slab, influencing the pattern of fluid influx into the mantle wedge. In this study, we calculate the fluid influx along the base of the mantle wedge, using the thermal modeling results and thermodynamic calculations based on *Perple_X*, and quantify fluid migration in the mantle wedge with the grain size and fluid influx distributions that are consistent with a given slab thermal structure.

Keywords: subduction zone, mantle wedge, aqueous fluid migration, grain size, slab dehydration, arc volcanism

Temperature dependence of seismic velocities in a antigorite serpentinite at 1 GPa

SHIRAI, Ryo^{1*} ; WATANABE, Tohru¹ ; YONEDA, Akira² ; MICHIBAYASHI, Katsuyoshi³

¹Department of Earth Sciences, Faculty of Science, University of Toyama, ²Institute for Study of Earth's Interior, Okayama University, ³Institute of Geosciences, Shizuoka University

Serpentines play key roles in subduction zone processes including water transport, seismogenesis, exhumation of high-pressure rocks, etc. Geophysical mapping of serpentized regions in the mantle wedge leads to further understanding of these processes. Seismic properties of serpentized peridotites are critical to interpretation of seismological observations. Antigorite is a major form of serpentine, which is stable to higher temperatures. The single-crystal elastic properties were recently revealed via Brillouin scattering technique (Bezacier et al., 2010; 2013). However, the temperature dependence of elastic properties is still poorly understood. We have measured elastic wave velocities in a antigorite serpentinite at high temperature and pressure conditions.

A black massive antigorite serpentinite was collected from the Nagasaki metamorphic rocks, western Japan. It is composed of antigorite (98.0 vol.%), diopside (1.5 vol.%) and magnetite (0.5 vol.%). Microstructural observation reveals an interpenetrating texture characterized by randomly oriented antigorite blades. Antigorite CPO data shows weak concentration of antigorite axes. Elastic wave velocities measured at 180 MPa shows very weak anisotropy in elasticity. Cylindrical samples (D=L=6mm) were made with ultrasonic machining.

Measurements were made at the pressure of 1 GPa and the temperature of up to 550 C, by using a piston-cylinder type high pressure apparatus at ISEI, Okayama University. The pulse reflection technique was employed for velocity measurement. One LiNbO₃ transducer with the resonant frequency of 5 MHz was used to transmit and receive ultrasonic signals. The length of the sample at high pressure and temperature conditions was estimated from the length of the recovered sample.

Both compressional and shear wave velocities linearly decrease with increasing temperature. The temperature derivatives are -3.6×10^{-4} (km/s/K) and -2.7×10^{-4} (km/s/K) for compressional and shear wave velocities, respectively. The temperature derivative of compressional wave velocity is close to that observed in the direction subparallel to antigorite *c*-axis (Yano et al., in prep.). The temperature dependence of *c*₃₃ might dominate that of the effective elastic constants of a randomly oriented polycrystalline aggregate. Applications to seismological observations will also be discussed in this presentation.

Keywords: seismic velocity, serpentinites, antigorite, subduction zone, fluid

Detection of structured water on quartz interface by Raman-FTIR spectroscopy and its evaluation by molecular dynamics

ISHIKAWA, Satoru^{1*} ; SAKUMA, Hiroshi² ; TSUCHIYA, Noriyoshi¹

¹Graduate School of Environmental Studies, Tohoku University, ²National Institute for Materials Science

Molecular structure of water in thin film shows different characteristics compared with that of free water. Thin film water was observed at mineral grain boundaries, and its structure might be influenced by mineral surface.

High temperature-pressure cell for micro-Raman and Fourier-transform infrared (FT-IR) spectroscopy have been developed to investigate molecular structure of thin film water at high temperature and pressure conditions. As a result of micro-Raman and FT-IR spectroscopic measurements of water, the broad peak around 3400 cm^{-1} , attributed to OH stretching vibration mode of water molecular, was observed at ambient temperature and pressure. The broad peak shifted to higher wavenumber with increasing temperature on metal reflector. Compared with the result of IR properties of water on metal reflector, IR properties of water on artificial quartz surface exhibit different trend: the broad peak contained the peak component of the lower wavenumber (around 3200 cm^{-1}), even at high temperature.

In addition, molecular dynamics simulations were performed under the conditions of the experiment using MXDORTO. In the simulation, the water of a few nanometers of quartz near the surface was structured. The distribution of water density was different from the free water. These properties are discussed in the hydrogen bond between water molecular and silanol (Si-OH) of quartz.

Keywords: Raman spectroscopy, IR spectroscopy, interfacial water, subcritical, quartz, molecular dynamics

Generation process of brecciated marble at Hiraodai karst, Kyushu, Japan

ISHIYAMA, Saya^{1*} ; ANDO, Jun-ichi¹ ; NAKAI, Shun'ichi² ; OTA, Yasuhiro³ ; DAS, Kaushik¹

¹Department of Earth and Planetary Systems Science, Hiroshima University, ²Earthquake Research Institute, the University of Tokyo, ³Kitakyushu Museum of Natural history & Human history

Geofluid is believed to be closely related to the seismic and volcanic activities. However, the detail relationship of geofluids with seismicity and volcanic activity is not studied properly through geological observations. We have found recently the brecciated marble widely distributed at Hiraodai karst plateau, Fukuoka Pref. This brecciated marble offers unique opportunity to study the relationship between geofluid and seismicity. Here, we shall explore the generation process of this brecciated marble through geological, microstructural and geochemical methods using polarization microscope, SEM, TEM, EPMA, microthermometric and MC-ICP-MS techniques.

The marble in Hiraodai karst plateau was thermally metamorphosed due to Cretaceous Hirao granodiorite intrusion. The brecciated marble occupies about 0.7 km x 1km of area in the central part of the karst. The main results of the present study are as follows.

- 1) The brecciated marble is composed of the rock fragments with variety of sizes ranging from millimeter to meter scale, and having angular to rounded shapes.
- 2) Numerous fluid inclusions are observed in the thin section of the brecciated marble.
- 3) TEM observation shows that the dense tangled dislocations are formed in calcite grains of the brecciated marble.
- 4) The homogenization and freezing temperatures of the fluid inclusions are about 240 deg C and 0 deg C, respectively.
- 5) The whole-rock and mineral separates (biotite and plagioclase) of Hirao granodiorite yields Rb-Sr isochron age of 129.4 +/- 2.4 Ma. Interestingly, Rb-Sr data of the fluid inclusions also lie on the Rb-Sr isochron of Hirao granodiorite.

The above-mentioned results of 1) and 2) suggest that the brecciation occurred by fluid infiltration and that the fragments were moved and rotated at very high speed. The result 3) demonstrates that the calcite grains of the brecciated marble experienced high stress. These three results together indicate that the brecciation process might generate seismic wave. On the other hand, the results of 4) and 5) suggest that the possible origin of the fluid inclusion is the released fluid from the Hirao granodiorite magma. Therefore, the brecciation of marble distributed at Hiraodai karst plateau was probably generated by magmatic fluid from Hirao granodiorite under high stress condition at 129.4 +/- 2.4 Ma ago.

Keywords: Brecciated rock, Hiraodai karst, Hirao granodiorite, Fluid inclusion, Rb-Sr isotope

Equation of state of topaz-OH in the subducted sediment under high pressure and high temperature

NIIZATO, Mizuki^{1*}; INOUE, Toru²; CAI, Nao²; SUENAMI, Hideki²; KAKIZAWA, Sho²

¹Department of Earth Sciences, Ehime University, ²Geodynamics Research Center, Ehime University

Dehydration reactions of hydrous minerals in the subducted sediment produce a H₂O-rich fluid which causes generations of magma, decreases of melting temperature of sediment, and variations of magma compositions. Topaz-OH [Al₂SiO₄(OH)₂], which is one of hydrous minerals, is considered to be existed in the sediment of the subducting slab. Topaz-OH is the end-member of natural topaz [Al₂SiO₄(OH,F)₂]. The stability field of topaz-OH extends to 1500 degree C at 5-10 GPa (Wunder *et al.*, 1993; Ono, 1998; Schmidt *et al.*, 1998). The equation of state (EoS) for the natural topaz has been also estimated (Komatsu *et al.*, 2003; Gatta *et al.*, 2003). However, the EoS of the end-member topaz-OH has not been performed yet. In this study, we performed *in situ* X-ray diffraction (XRD) experiments under high pressure and high temperature for determining the thermal elastic properties of topaz-OH.

The starting material of topaz-OH was synthesized at 10 GPa and ~1000 degree C from the quench experiment using multi-anvil apparatus. The high pressure (3-8 GPa) and high temperature (up to 800 degree C) *in situ* XRD experiments were carried out using MAX80 installed at beam-line NE5C at PF-AR, KEK, Japan. These XRD patterns were collected by the energy dispersive method. Thermal elastic properties were calculated from EoS fit v5.2 software (Angel, 2000) using 3rd order Birch-Murnaghan EoS.

From *in situ* XRD experiments, we successfully determined thermal elastic properties using all-data for fixed K'=4 as below: V₀=354.7(1) Å³, K₀=169.8(22)GPa, (dK_T/dT)_P=-0.013(7) GPaK⁻¹, a₀=1.61(23)×10⁻⁵K⁻¹, b₀=1.36(41)×10⁻⁸K⁻². From the detailed analysis of compression data, we found the change of the compression properties near 7 GPa. This change was also seen in a- and b-axis. Therefore we re-calculated the thermal elastic properties using two data sets: (I) below 7 GPa (II) above 7 GPa at room temperature. These calculation results from low pressure data show V₀=355.2(1) Å³, K₀=160.1(2)GPa, however those from the high pressure data show V₀=356.5(9) Å³, K₀=153.1(89) GPa (K'=4 fixed). Compared to the natural topaz, topaz-OH shows relatively large volume and bulk modulus. This shows that the volume and bulk modulus increase with increasing OH content. Compared bulk modulus with density, topaz-OH locates near the line for Birch's law and indicates large bulk modulus and density as same as Phase D [Mg₂SiO₄(OH)₂]. We suggest that high density topaz-OH enhances the slab subduction and transports water to deeper earth's interior.

Keywords: topaz-OH, high pressure hydrous phase, subducting slab, equation of state, synchrotron X-ray in-situ experiment

Water content in arc basaltic magma in northeast Japan and Izu-Mariana arc estimated from melt inclusions in olivine and

USHIODA, Masashi^{1*}; IKEGUCHI, Naoki¹; TAKAHASHI, Eiichi¹

¹Dept. Earth and Planetary Sciences, Tokyo Institute of Technology

Primitive arc basalt magma is generated by partial melting of sub-arc mantle with adding aqueous fluid which was derived from dehydration of subducting slab. Aqueous fluid has profound effects on melting temperature of the mantle, crystallization pathways of generated magmas, and explosivity of magmas. Precise estimation of H₂O content in arc basalt magma is important to evaluate the effect of water on generation, differentiation, and eruption of magmas in subduction zones. We estimated variation of water content of arc basaltic magmas in the northeast Japan arc and the Izu-Mariana arc using a simple plagioclase phenocryst hygrometer and melt inclusion analysis of olivine phenocrysts.

A simple plagioclase phenocryst hygrometer was constructed by high-pressure and high temperature experiments using internally heated pressure vessels: SMC-2000 and SMC-5000 installed at the Magma Factory, Tokyo Tech (Ushioda et al., 2013, VSJ fall meeting). High-pressure and high-temperature experiments were conducted for relatively primitive basalt from Miyakejima volcano under hydrous conditions. OFS (Ofunato scoria: Tsukui et al., 2001; Niihori et al., 2003) is one of the most primitive basalt in the last 10,000 years. All experiments were conducted near the liquidus of plagioclase (\pm magnetite) and therefore the composition of melt is essentially the same as the starting material. H₂O content of melt was calculated by weight ratio of melt using mass balance calculation of all phases assuming that water was concentrated only in melt. Partition coefficient $K_D^{pl-melt}{}_{Ca-Na}$ is proportional to H₂O content in melt. In the experimental conditions, both pressure and temperature effects are negligible.

We then chose geochemical data sets of relatively primitive basaltic rocks (with no evidence of magma mixing) and most frequent Ca-rich plagioclase phenocrysts from 15 arc basaltic volcanoes, which includes both frontal arc volcanoes and rear-arc volcanoes from literature. In 15 volcanoes, plagioclase phenocrysts of high anorthite content (An>90) are commonly observed, whereas plagioclase phenocrysts in rear arc volcanoes usually have lower anorthite content (90>An>80). Estimated H₂O content of basaltic magma is 3 wt.% H₂O or higher.

We also analyzed H₂O content of melt inclusions in olivine phenocrysts using FTIR micro reflectance measurement (Yasuda, 2011) and FTIR micro transmission measurement (absorption coefficient: Yamashita et al., 1996) in order to compare H₂O content between melt inclusion analysis and this simple plagioclase phenocryst hygrometer. For example, melt inclusions of olivine phenocrysts in scoria from Ko-Fuji volcano had up to 3.7 wt.% H₂O which was consistent with estimate from our simple plagioclase phenocrysts hygrometer. In Miyakejima volcano, melt inclusions of olivine phenocrysts from OFS contained up to 3.3wt.% H₂O although H₂O content was 5.2 wt.% estimated from this hygrometer. In either case, basaltic magmas in volcanic front have 3 wt.% H₂O or higher.

Keywords: water in magma, melt inclusion, equilibrium between plagioclase and melt

DEM simulation on fracturing induced by hydration and dehydration reactions

OKAMOTO, Atsushi^{1*} ; SHIMIZU, Hiroyuki²

¹Graduate School of environmental Studies, Tohoku University, ²Institute of Fluid Science, Tohoku University

Dehydration and hydration reactions play significant roles on the global water circulation in the solid Earth, and cause drastic change in the mechanical properties of the subduction zone interface. Progress of both reactions requires an effective transport of water (release or supply) between the reaction sites and outer system, and are commonly characterized by large changes in solid volume, porosity, and fluid pressure. Reaction textures with fracturing are commonly observed both in hydration and dehydration hydration reactions. However, the dynamic relationship among reactions, fluid transport and deformation (fracturing, plastic deformation) is too complicated to be understood solely by observations of natural occurrences.

In the present study, we carried out numerical simulations on fracturing induced by hydration or dehydration reactions by using distinct element method (DEM). At first, we consider a dehydration reaction like a dehydration of serpentine. In the model, the following factors are introduced: (1) pressure dependence of reaction rate, (2) grain boundary as weak and water-saturated region, and that (3) mineral grains become permeable after fracturing or reacted. In this model, reaction rate drastically decreases with progress of dehydration reaction, when fluid cannot escape from the system.

We examined two rock systems; one is composed of reactive minerals (uniform-reactive system) and the other one is composed of reactive minerals embedded in unreactive matrix minerals (reactive minerals in matrix system). In both systems, one is drain-boundary, whereas all the others are undrain-boundary. The spatial variation in fractures and progress of reactions are contrasting between the two systems. In the uniform-reactive system, fracturing does not occur and reactions uniformly occur from the drain-boundary, because fluid effectively escapes through newly-produced pore-network. In contrast, the reactive-mineral-in-matrix-system, the fracture network is produced among the reactive grains, and heterogeneous distributions of reaction progress was produced in the rocks. We will further discuss the key parameters to controls the fracture patterns and difference between hydration and dehydration reactions.

Keywords: hydration, dehydration, fracturing, distinct element method